Original Article

Reduction of FoxP3$^+$ Tregs by an immunosuppressive protocol of rapamycin plus Thymalfasin and Huaier extract predicts positive survival benefits in a rat model of hepatocellular carcinoma

Lin Zhou[1,2,3#], Li-Chao Pan[2#], Yong-Gen Zheng[3], Xin-Xue Zhang[1], Zhi-Jia Liu[3], Xuan Meng[2], Hai-Da Shi[2], Guo-Sheng Du[3], Qiang He[1]

[1]Department of Hepatobiliary and Pancreaticosplenic Surgery, Beijing ChaoYang Hospital, Capital Medical University, Beijing 100020, China; [2]Department of (Second) Hepatobiliary Surgery, the 1st Medical Center of Chinese PLA General Hospital, Beijing 100853, China; [3]Departmentof Hepatobiliary Surgery, the 8th Medical center of Chinese PLA General Hospital, Beijing 100091, China

Contributions: (I) Conception and design: L Zhou, GS Du, Q He; (II) Administrative support: None; (III) Provision of study materials or patients: YG Zheng, LC Pan; (IV) Collection and assembly of data: YG Zheng, XX Zhang, HD Shi, ZJ Liu; (V) Data analysis and interpretation: L Zhou, XX Zhang, ZJ Liu; (VI) Manuscript writing: All authors; (VII) Final approval of manuscript: All authors.

[#]These authors contributed equally to this work.

Correspondence to: Prof. Guo-Sheng Du. A-17 Heishanhu Road, Haidian District, Beijing 100091, China. Email: duguosheng309@126.com; Prof. Qiang He. 8 GongtinanRoad, Chaoyang District, Beijing 100020, China. Email: heqiang349@sina.com.

Background: Investigate immunoregulation and anti-tumor immunity of FoxP3$^+$Tregs after treatment with rapamycin (RAPA/SRL) plus thymalfasin (Zadaxin) and Huaier extract (PS-T) in a hepatocellular carcinoma (HCC) rat model simulating HCC relapse after liver transplant (LT).

Methods: We successfully established a rat model simulating HCC relapse after LT using an optimized chemical induction method with TACROLIMUS, methylprednisolone, and diethylnitrosamine as identified by visible liver nodules and hematoxylin-eosin staining. The model rats were then treated with RAPA, Zadaxin, and PS-T. Immune status changes were analyzed by flow cytometry, and protein expression of Akt and mTOR was determined by western blotting. Cytokines were measured by ELISAs.

Results: Combined therapy by RAPA plus Zadaxin and PS-T obviously alleviated hepatic pathological changes and significantly decreased the levels of FoxP3$^+$Tregs in peripheral blood, the spleen, and the liver ($P<0.05$) and expression of mTOR protein ($P<0.01$) in the liver, obviously improved survival time ($P=0.02$). Moreover, the levels of CD8$^+$T cells were increased significantly to almost normal levels ($P<0.05$) in comparison with no SRL monotherapy protocols. Inhibitory cytokines were also decreased in accordance with FoxP3$^+$Tregs. Significant decreases of IL-10 and TGF-β were observed after SRL-based therapy ($P<0.01$) in comparison with the other groups. Serum alpha fetoprotein (AFP) and vascular endothelial growth factor (VEGF) levels were also decreased significantly ($P<0.05$). FoxP3$^+$Tregs showed a negative correlation with CD8$^+$ and CD4$^+$/CD8$^+$T cells and a positive correlation with AFP, and VEGF ($P<0.05$).

Conclusions: SRL-based therapy reduces FoxP3$^+$Tregs to decrease secreted inhibitory cytokines which may enhancement the viability and number of CD8$^+$T cells to exert anti-tumor effects that are mainly mediated through the AKT-mTOR signaling pathway.

Keywords: Regulatory T cells (Tregs); rapamycin; hepatocellular carcinoma (HCC); tumor immunology; rat model; immunosuppression

Submitted Dec 02, 2019. Accepted for publication Feb 14, 2020.
doi: 10.21037/atm.2020.03.129
View this article at: http://dx.doi.org/10.21037/atm.2020.03.129

Introduction

Hepatocellular carcinoma (HCC) is one of the five most common malignancies (1) and the second and third most frequent cause of cancer deaths worldwide in men and women, respectively (1-3). The incidence of HCC has continually increased in both Western and Asian countries over the past 10 years (3,4). Apart from liver resection, liver transplantation (LT) is currently recognized as the most effective therapeutic approach to potentially eliminate HCC lesions (5). Despite a restrictive patient selection policy, the recurrence rate of HCC after LT is still 3–25% and drastically affects long-term survival (6-10). Although there is currently no consensus on the most suitable method to prevent relapse and the best therapeutic approach to avoid tumor recurrence; re-resection, radiofrequency ablation, and transcatheter hepatic arterial chemoembolization are alternative options. The 2019 ASCO has recommended lenvatinib as the first-line treatment for advanced liver cancer over sorafenib that was the only efficacious adjuvant therapy for tumor relapse previously (11,12), but the results remain unsatisfactory. Therefore, studies on tumor recurrence and cancer immunity after organ transplantation are desired.

$CD4^+CD25^+FoxP3^+$ regulatory T cells ($FoxP3^+$Tregs) have been demonstrated to perform important functions in tumor immunity and graft immune tolerance (13). Increasing numbers of studies have indicated that a preoperative increased level of $FoxP3^+$Tregs in HCC patients is often associated with poor survival and a high risk of tumor relapse (14,15). Although $FoxP3^+$Tregs induce immune tolerance, recent studies have demonstrated that a high frequency of $FoxP3^+$Tregs after LT for HCC may be associated with an increased risk of tumor recurrence and reduced long-term survival benefits. Thus, $FoxP3^+$Tregs might play a contradictory role in immune tolerance induction and tumor recurrence prevention of HCC after LT. Investigation of a suitable immunosuppressive therapy by a "killing two birds with one stone" approach that effectively reduces graft rejection and avoids the high relapse risk associated with long-term application of TACROLIMUS (16) is an important research focus. The recent "SiLIVER" study demonstrated that rapamycin (RAPA/SRL) is an efficacious immunosuppressive drug and anti-neoplastic agent for LT patients with excellent clinical safety and efficacy (17). Our previous study also found that SRL plus Huaier granule (PS-T) and Zadaxin treatment of patients with LT for advanced HCC reduces $FoxP3^+$Tregs (18), which provides evidence supporting SRL selection and TACROLIMUS replacement therapy for HCC after LT.

Trametes robiniophila Murr. in traditional Chinese medicine (TCM) has been used for more than 1,600 years as a medicinal fungus for the treatment of inflammation and cancer in China (19,20). Huaier granule (PS-T) is a representative TCM against cancer as an adjuvant drug for chemo-radiotherapy with excellent clinical efficacy against liver, lung, gastric, and breast cancers (19-22). PS-T is a multi-target drug with effective ingredients of proteoglycans that improve immune functions, especially those of effective T and natural killer cells, which kills tumor cells (22,23). Furthermore, Huaier inhibits the tumorigenic capacity of cells and increases the sensitivity of cells to rapamycin via the mTOR signaling pathway (22,24). Most transplant physicians are in favor of SRL replacement therapy for HCC patients' post-transplantation (25). By application of RAPA/SRL plus Zadaxin and PS-T (combined therapy/SRL-based therapy) for terminal HCC patients after LT, we obtained excellent clinical prognoses with long-term survival benefits and a delayed tumor relapse time (18) after a 5-year follow-up. The treatment even regulated $CD8^+$T cells and the ratio of $CD4^+/CD8^+$T cells by Zadaxin and demonstrated its efficacy and safety (18,26).

$CD8^+$T cells are the main effective cells in anti-tumor responses and graft rejection (27). The balance between each subgroup of T cells, especially the dynamic equilibrium of $CD4^+/CD8^+$T cells, contributes to maintaining the stability of cellular immune functions and inhibition of tumor growth (28-31). $FoxP3^+$Tregs exert anti-tumor and immune regulatory effects through direct and indirect interactions with $CD4^+$ and $CD8^+$T cells (13,14,32). A high level of $FoxP3^+$Tregs might induce tolerance inpatients after LT (33), but it can lead to a decreased level and hypoergia of $CD8^+$T cells (34-36). Conversely, relatively low levels of $FoxP3^+$Tregs favor prevention of tumor relapse, but might lead to rejection (34,35). Interestingly, SRL-based therapy in our center has achieved a relatively promising state associated with a comparatively low frequency of $FoxP3^+$Tregs with no effect on the rejection rate, which resolves these issues (18), but the detailed anti-tumor and immunity mechanisms are not fully understood. To explore whether the combined therapy regulates T cell immunity via the mTOR signaling pathway, we conducted this study under an immunosuppression environment to establish a simulative model of HCC relapse. In the present study, we mainly investigated regulatory mechanisms of $FoxP3^+$Tregs

in SRL-based therapy compared with other groups which was accepted no replace with SRL therapy, focusing on anti-tumor effects.

Methods

Animals and experimental groups

Sprague-Dawley (SD) male rats aged 6–8 weeks and weighing 180–220 g were obtained from the Animal Experiment Center of the Military Academy of Medical Sciences. The animal experiments were approved by the 8th Medical Center of Chinese PLA General Hospital Medical Animal Ethics Committee. Animals were housed and treated in accordance with the Animal Welfare Act and Institutional Guidelines for the Care and Use of Laboratory Animals.

Seventy-two SD rats were randomly divided into six groups using a random number table as follows: Combined group/SRL-based therapy (A), SRL/RAPA group (B), Thymalfasin/Zadaxin group (C), Huaier extract/PS-T group (D), HCC model group (E), and blank group (control) (F).

Establishment of a rat model to simulate HCC recurrence after LT and study protocol

A rat model of HCC recurrence after LT was established with optimization and improvement according to previous studies (37-40) and our preliminary experimental results. Briefly, chemical agents were used to induce cancer and establish the SD rat model. First, an immunosuppressive environment was simulated by combined application of TACROLIMUS at 0.08 mg/kg/day plus methylprednisolone at 20 mg/kg/day, and methylprednisolone was withdrawn after 7 days. This regime was sustained for 1 month to generate an immunosuppressive microenvironment. Then, TACROLIMUS was replaced with SRL in groups A and B, whereas the other groups (C–F) were treated with normal saline (NS). Chemical induction of cancer with diethylnitrosamine (DEN) was then performed by intraperitoneal injection and a low concentration provided *ad libitum* in drinking water as the basic induction protocol. A 100 mg/kg preparation of DEN in sterile water was injected on the first day of every month. A 0.075 mg/mL preparation of DEN in sterile water was freely available to drink on the second week of every month. DEN in drinking water was provided on days 1, 3, and 5 of every week and sterile water was provided on the other days. This protocol was continued for at least 3 months or until death.

The drug intervention was prepared in advance and started at 2 months after initiation of DEN treatment. SRL was administered by gavages at a dose of 0.5 mg/kg once a day, PS-T was administered by gavages at 1 mg/mL three times per day, and Zadaxin was administered as a 0.35 mg/kg subcutaneous injection for 10 days and then twice weekly at the same dose. Rats in group A received combined drugs, groups B–D received individual drugs, group E was the tumor rat which treated replaced drug with NS, and group F was just immunosuppressed rat which had no intervention. Drug treatment continued until the end of the experiment or death.

Reagents and drugs

APC-conjugated anti-rat CD3, PE-conjugated anti-rat CD8, FITC-conjugated anti-rat CD4, PE-conjugated anti-rat CD25, and APC-conjugated anti-rat FoxP3 antibodies, Foxp3 Staining Buffer Set (BD Pharmingen, USA); AFP and VEGF ELISA kits (R&D Systems, USA); rat vascular endothelial growth factor (VEGF) immunohistochemistry (IHC) kit (Proteintech, USA); RMPI-1640, DMEM, and FBS (Gibco, USA); diethylnitrosamine (DEN; Sigma, USA); rapamycin (Wyeth Pharmaceuticals Company, USA); Huaier extract (Gaitianli Medicine Co.Ltd., China); Thymalfasin (Patheon Italia S.p.A, Italy); Tacrolimus (Astellas Pharma Inc., Japan).

Specimen collection and preparation

General samples

Peripheral blood (PB) was collected each month. All rats were sacrificed by cervical dislocation under general anesthesia. After obtaining images, PB, liver and spleen samples were collected in sterile RMPI-1640 medium.

Preparation of lymphoid cell suspensions of the spleen and liver

Spleen and liver lymphoid cell suspensions were prepared by mincing the rat spleen and liver on a wire mesh. The cells were pooled and passed through a nylon mesh to remove cell clumps with repeatedly washed in RPMI-1640 medium. The cell suspension was transferred to a 15-mL centrifuge tube and centrifuged at 1,200 rpm for 10 min. The supernatant was discarded and FBS was added, followed by blending in a beater to obtain a single cell suspension. The suspensions of spleen and liver cells were purified by density gradient centrifugation at 1,800 rpm for

30 min. The cloudy cell layer in the middle was collected, washed withRPMI-1640 medium, and centrifuged again. The supernatant was discarded, and the cells were resuspended in RPMI-1640 medium. Cells were stained with trypan blue, and samples with >90% live cells were used for experiments.

Preparation of tissue histopathological specimens

Liver tissue of rats with suspected tumors was fixed in formalin, dehydrated, embedded, sectioned at 5 μm thicknesses, stained with hematoxylin-eosin (HE), and observed and photographed under a microscope.

Measurement approaches

Flow cytometric analysis of the Foxp3$^+$Treg, CD3$^+$CD4$^+$, and CD3$^+$CD8$^+$T cell populations was performed for control, PB, and lymphoid cell suspensions of the spleen and liver. Serum AFP and VEGF were analyzed by ELISA kits, and immunohistochemistry of VEGF was performed with the VEGF IHC kit. HE and IHC staining was observed and images under an IX-90 confocal laser scanning microscope (Olympus Optical, Tokyo, Japan) at ×10 and ×20 magnifications.

VEGF IHC was followed these steps, the 10% formalin fixed tissues embedded in paraffin, microtome section with 5 μm, heated at 60 ℃ on slides warmer for 30 min, dewaxing, 3% H_2O_2 inactivation, pretreated in a microwave at 100 ℃ for 20 min, and closed antibody incubation for 30 min. Next, incubated with primary antibodies to VEGF (1:100, Abcam, USA) for night. Incubation with second antibody to PV-9000 kits (OriGene Technologies, USA) for 60 min, IHC staining was detected by an Olympus microscope system (Japan) and DAB kit (Vector, USA).

Protein isolation and western blotting

Total protein was prepared at 4 ℃ lysis buffer of cancer cells isolated from tumor nodes using trypsinization. Then, the protein purity was determined by a BCA assay, according to the R&D manufacturer's instructions. Western blotting was performed by preparation of a separation gel and samples, electrophoresis, membrane transfer, blocking, antibody incubation, development, and fixation.

Statistical analysis

All measurement data are presented as the mean ± SD and analyzed with SPSS 19.0 software. Statistical significance was evaluated using the unpaired Student's *t*-test. The Kaplan-Meier method was used to calculate survival curves, followed by log-rank analysis. Comparisons among more than three groups were performed by analysis of variance. Quantitative data were compared by chi-squared tests. Correlation analysis between continuous variables was based on Pearson's analysis. P<0.05 was considered as statistically significant.

Results

Rat livers pathological morphology

Compared with the liver of normal rats (group F), livers of group E showed severe changes with an uneven surface, jagged rim, and cirrhosis as well as multiple nodular lesions with maximum size of almost 10 mm (*Figure 1*). In group A, the color and luster of the liver was essentially normal with no obvious cirrhosis or nodules. There were small nodules with slight cirrhosis in group B, and these lesions were alleviated in groups C and D (*Figure 1A*).

The results of HE staining were consistent with the specimen observations. Pathology in group E indicated that the liver lobular structure had disappeared, and the tumor cells showed significant atypia with various cell sizes and shapes, and their nuclei were large and deeply stained and arranged densely (*Figure 1B*). Microscopic analysis showed that 91.7% (11/12) and 75% (9/12) of rats in group E displayed signs of HCC and visible liver nodule lesions, respectively, at the experiment endpoint. The other groups had minor lesions in only a few rats with 16.7% (2/12) in group A, 33.3% (4/12) in group B, 41.7% (5/12) in group C, and 33.3% (4/12) in group D (*Figure 1C*). These findings demonstrated that the simulative animal model was successfully established and conformed to the pathological manifestations of HCC recurrence after LT.

FoxP3$^+$Tregs and their influence on CD4$^+$and CD8$^+$T cells

Comparison of FoxP3$^+$Treg cells

FoxP3$^+$Treg cells in peripheral blood

The percentages of FoxP3$^+$Tregs among CD4$^+$T cells and lymphocytes was 5.0%±0.9% and 2.03%±0.45%, respectively (*Table 1*, *Figure 2*). Compared with group F, there was a significant increase of FoxP3$^+$Tregs in group E (9.71%±1.03%, P<0.01) and significant decrease ingroup A (3.84%±0.58%, P<0.01) (*Figure 2A*,*B*). Moreover, compared with groups E (9.71%±1.03%), B (5.15%±0.75%), C (5.24%±0.64%), and D (5.11%±0.82%), the difference in

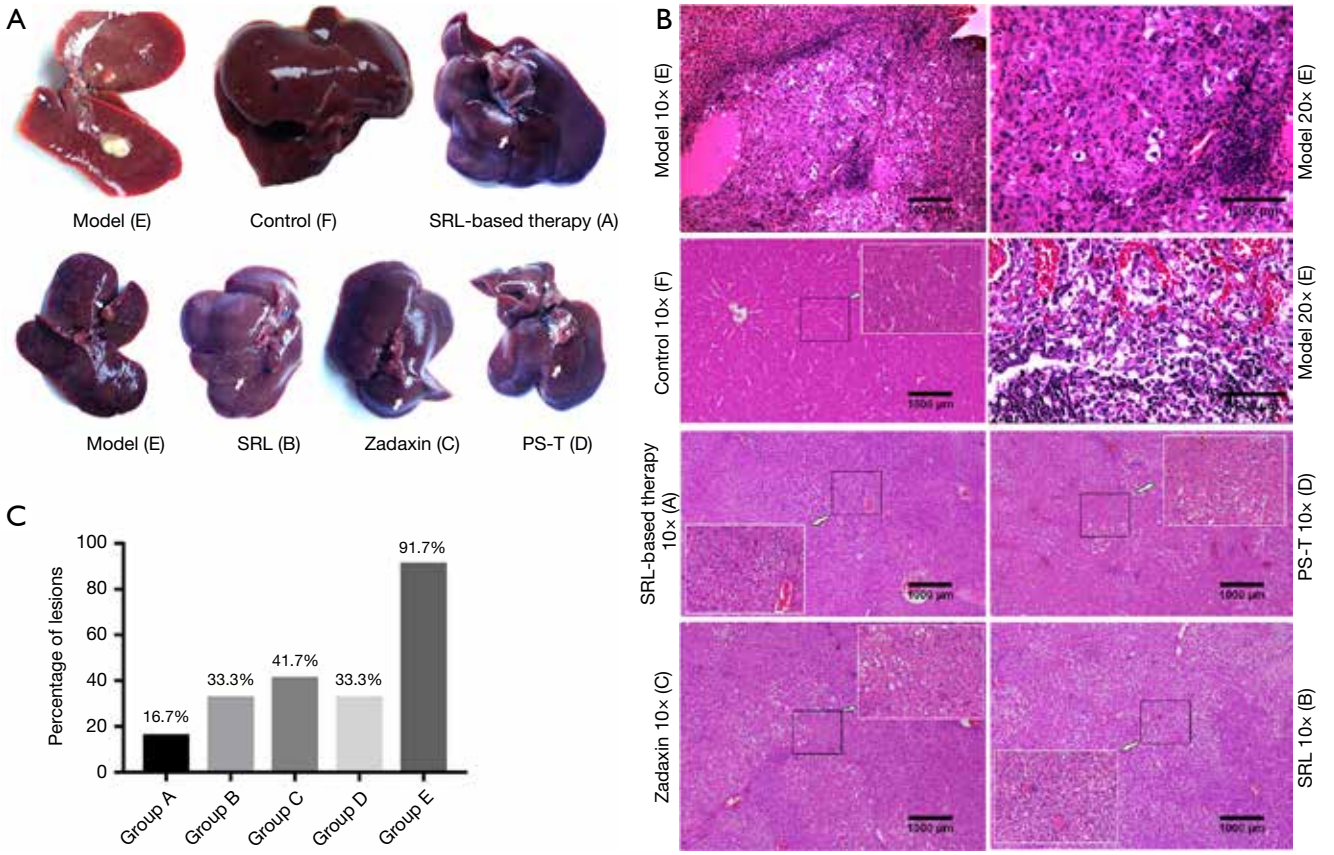

Figure 1 The Pathological morphology of rat liver in each experimental group. (A) The liver pathological lesions photos to the naked eye of each experimental groups shown by arrows, the rats of HCC model group displayed tumor nodules, 5–10 mm (model group), and the tissue lesions were gradually reduced with the drug intervention. (B) The pathological results of HE stains for each group which shown with 10× and 20× images. (C) Histogram of tumors in each group. Group A, SRL-based therapy; Group B, SRL/RAPR; Group C, Zadaxin; Group D, PS-T; Group E, Model; Group F, Control.

Table 1 The levels of FoxP3$^+$Treg of PB, liver and spleen in different groups

Groups	PB (n=12)			Liver (n=12)			Spleen (n=12)		
	means	SD	[a]P value	means	SD	[b]P value	means	SD	[c]P value
Group A	3.84	0.58	<0.001	2.79	0.59	0	4.26	0.34	0.042
Group B	5.15	0.75	<0.001	3.94	0.73	0	5.40	0.61	0.380
Group C	5.24	0.64	0.005	4.33	0.78	<0.001	5.75	0.81	0.101
Group D	5.11	0.06	0	3.75	0.49	0	5.39	0.58	0.110
Group E	9.71	1.03	0	4.77	0.87	0.065	5.99	1.98	0
Group F	2.03	0.38	0.049	1.69	0.42	0.004	2.64	0.96	0.053

[a]P value: FoxP3$^+$Treg in PB *vs.* Liver; [b]P value: FoxP3$^+$Treg in Liver *vs.* Spleen; [c]P value: FoxP3$^+$Treg in PB *vs.* Spleen. Group A, SRL-based therapy group; Group B, Rapamycin/Sirolumus group; Group C, Thymalfasin group; Group D, Huaier extract group; Group E, HCC model group; Group F, Control.

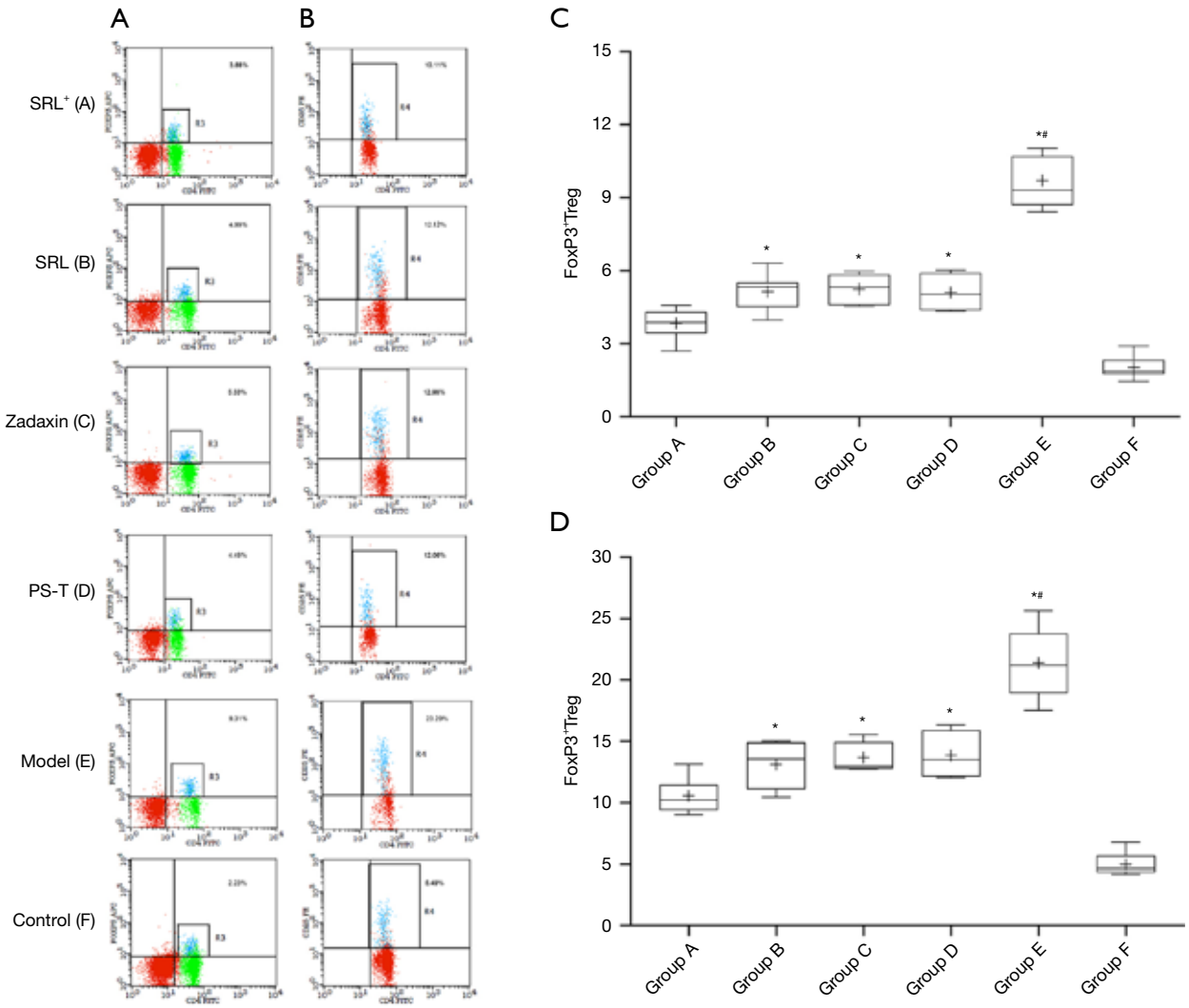

Figure 2 The FoxP3$^+$Treg of each group in peripheral blood (PB). (A) Scatter diagram of FoxP3$^+$Treg in lymphocyte and (B) in CD4$^+$T cells detected by flow cytometry; (C) the FoxP3$^+$Treg in lymphocyte (analysis by ANOVA); (D) the level of FoxP3$^+$Treg in CD4$^+$ T cells for each group, (analysis by ANOVA). *P<0.01, compared with group A; $^{\#}$P<0.01, compared with group F. Group A, SRL$^+$; Group B, SRL/RAPR; Group C, Zadaxin; Group D, PS-T; Group E, Model; Group F, Control.

group A was statistically significant (P<0.01) (*Figure 2C,D*). The difference among no SRL monotherapy groups (B–D) was not statistically significant (P>0.05) (*Table 1*, *Figure 2A-D*).

FoxP3$^+$Treg cells in the spleen and liver

Except for group E, the trends in changes of FoxP3$^+$Tregs in the spleen and liver of the other four groups was essentially in accordance with the higher level in the spleen than in PB (*Figure 3*), but the differences were not statistically significant (P>0.05) (*Table 1*, *Figure 3A,B*). However, the level in the liver was notably lower than that in PB (P<0.05) (*Table 1*, *Figure 3A,B*). For group E, the FoxP3$^+$Treg level in PB was notably higher than that in the spleen and liver with a statistical significance (P<0.05) (*Table 1*, *Figure 3A,B*).

Influence of FoxP3$^+$Tregs on effective T cells

CD4$^+$and CD8$^+$T cells in peripheral blood, the spleen, and liver

Compared with group E, there was a significant increase of CD8$^+$T cells in groups A–C (P<0.05) (*Figure 4*). Interestingly, compared with groups B–D, there also was a notable increase of CD8$^+$T cells in group A, and the difference between group A and each of these groups was

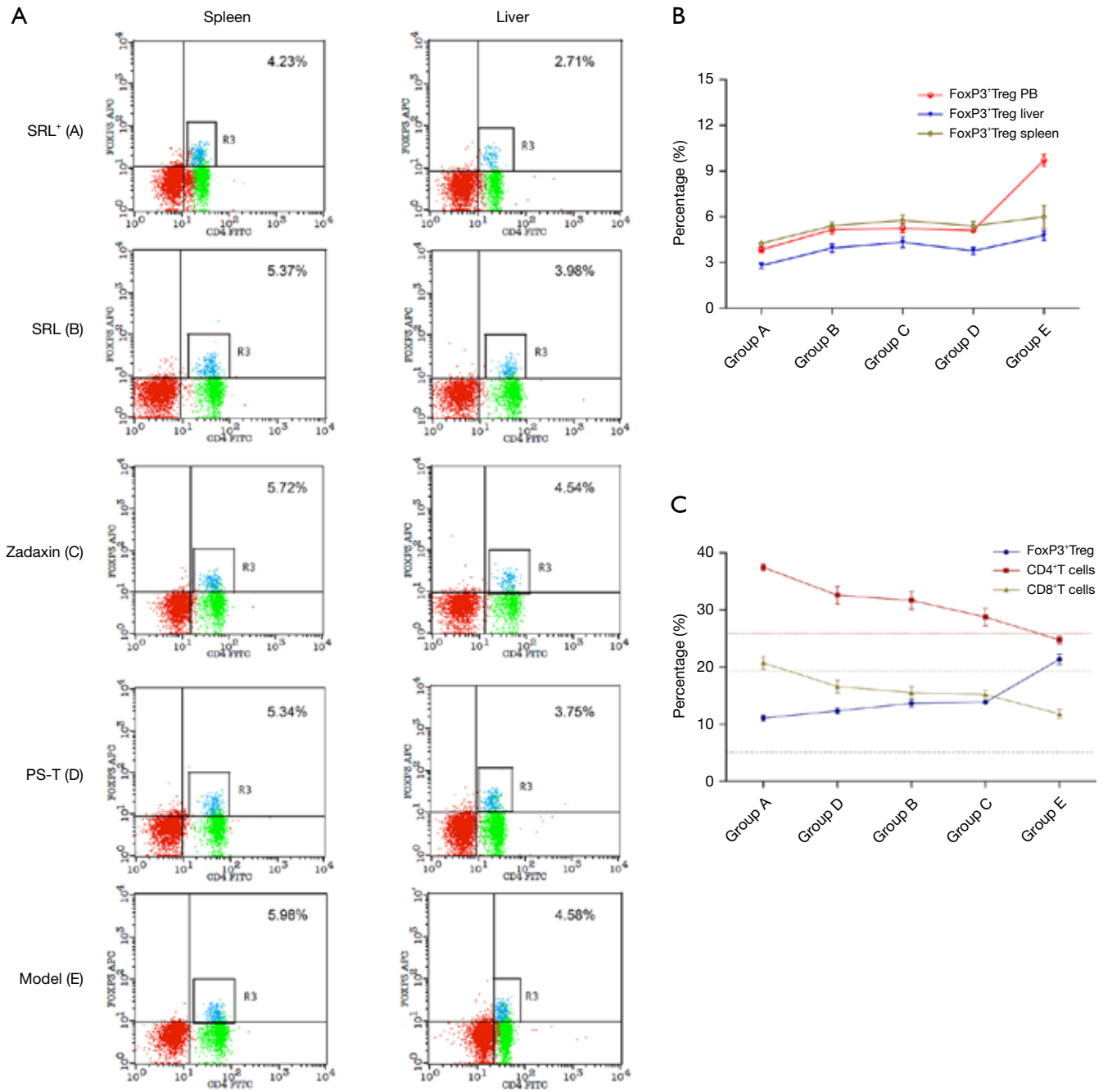

Figure 3 The levels of FoxP3$^+$Treg in different tissues for rats in the different groups. (A) Scatter diagram of flow cytometry of the FoxP3$^+$Treg in spleen and liver. (B) Multi-group analysis of ANOVA for FoxP3$^+$Treg expression in different tissues. (C) Changes of FoxP3$^+$Treg and CD4$^+$ as well as CD8$^+$ T cells in PB of different groups. Group A, SRL$^+$; Group B, SRL/RAPR; Group C,Zadaxin; Group D, PS-T; Group E, Model.

statistically significant (P<0.05) (*Figure 4A,C*). The increase of CD4$^+$T also had a statistical significance but was slightly lower than that of CD8$^+$T cells (*Figure 4B,D*).

There was a similar trend of effective T cells in the spleen and liver of group A. Significant decreases of CD8$^+$ and CD4$^+$T cells were found in group E (*Figure 4A,B,E,F*).

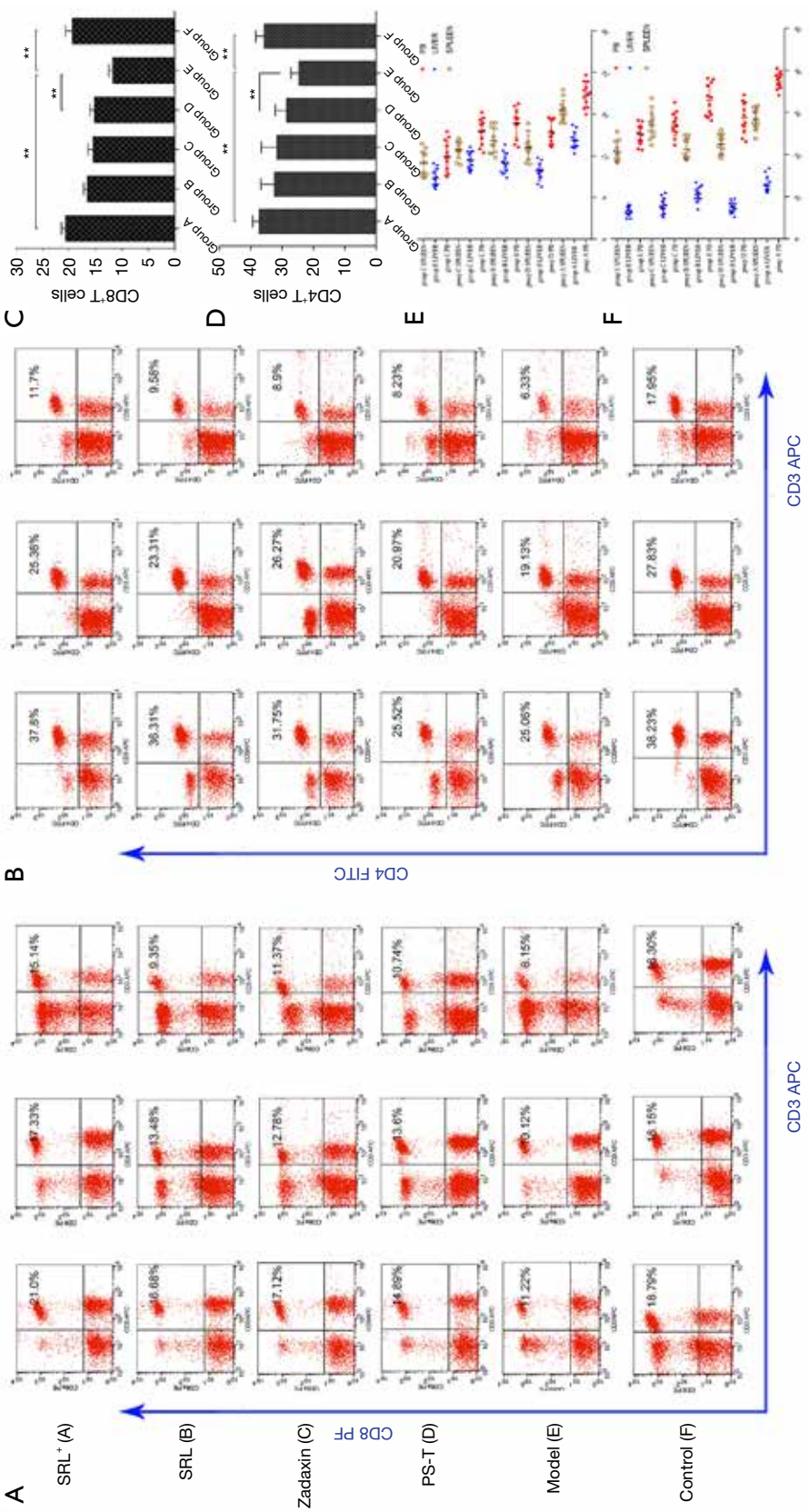

Figure 4 The expression of $CD4^+$ and $CD8^+$T for each group in different tissues. (A) The levels of $CD8^+$T cells for each group in different tissues for rats in the different groups with Scatter diagram of Flow cytometry. (B) The levels of $CD4^+$T cells for each group in different tissues for rats in the different groups with Scatter diagram of Flow cytometry. The left column in PB, the middle column was in spleen, the right column was in liver. (C) Analysis of ANOVA for $CD8^+$T cell expression of different groups in PB (**P<0.01, compared with group E). (D) Analysis of ANOVA for $CD4^+$T cell expression of different groups in PB (**P<0.01, compared with group E). (E) Scatter plot of $CD8^+$T cells in different tissues various from different groups. (F) Scatter plot of $CD4^+$T cells in different tissues various from different groups (rather higher level in PB, middle in the spleen and markedly lower in the liver for each group, analysis by ANOVA, P<0.01). Group A, SRL^+; Group B, SRL/RAPR; Group C, Zadaxin; Group D, PS-T; Group E, Model; Group F, Control.

Table 2 The correlation ship of FoxP3$^+$Treg between CD4$^+$T cells, CD8$^+$T cells and CD4$^+$/CD8$^+$T cells in PB

Groups	Treg and CD4$^+$T cells		Treg and CD8$^+$T cells		Treg and CD4$^+$/CD8$^+$T cells	
	r	P	r	P	r	P
Group A	−0.979	0.000	−0.955	0.000	−0.884	0.002
Group B	−0.977	0.000	−0.946	0.001	−0.906	0.005
Group C	−0.931	0.021	−0.978	0.004	−0.945	0.015
Group D	−0.908	0.033	−0.985	0.002	−0.897	0.039
Group E	−0.998	0.000	−0.947	0.001	−0.964	0.000
Group F	−0.935	0.000	−0.648	0.043	−0.972	0.000

Group A, SRL-based therapy group; Group B, Rapamycin/Sirolumus group; Group C, Thymalfasin group; Group D, Huaier extract group; Group E, HCC model group; Group F, Blank group.

After drug intervention, the percentages of CD8$^+$ and CD4$^+$T cells were improved in each group. This indicated that the inhibitory effect of FoxP3$^+$Tregs was most significant in group E, which was in accordance with the data for PB (*Figure 3C*, *Figure 4A-F*).

Inhibitory effect of FoxP3$^+$Treg cells

It has been shown that a high level of FoxP3$^+$Tregs has a significant inhibitory effect on CD4$^+$ and CD8$^+$T cells, as displayed in group E. In contrast, the inhibitory effect of a low level of FoxP3$^+$Tregs in the other groups was significantly decreased after drug application, which was most obviously displayed in group A (*Figure 3C*).

Correlation analysis of FoxP3$^+$Tregs and effective T cells

The ratio of CD4$^+$/CD8$^+$T cells in group A was 1.85±0.26, which was closest to that in group F (1.96±0.41). There was a marked decrease of the ratio in group E (1.44±0.27), and no obvious increase in groups B–D with mean values of 2.09±0.40, 2.04±0.10, and 1.90±0.30, respectively. Correlation analysis indicated a negative correlation between FoxP3$^+$Tregs and CD4$^+$/CD8$^+$T cells, and the ratio of CD4$^+$/CD8$^+$T cells (*Table 2*).

Tumor marker and cytokine analysis

Alpha fetoprotein secretion

Alpha fetoprotein (AFP) is a highly specific and highly sensitive tumor marker for primary liver cancer. Its cutoff value is usually 20 μg/L and has a strong diagnostic value at >400 μg/L or rising constantly. AFP is usually combined with imaging findings for the diagnosis of HCC. Serum AFP levels in groups B–E were increased significantly compared with those in group F (Blank group) (P<0.01) (*Figure 5*). In addition, there was a significant decrease of the AFP level in group A compared with that in group E (P<0.05) (*Figure 5A*). Although the AFP level in no SRL monotherapy groups was lower than that in group E (P<0.01), there was no significant difference among the monotherapy groups (P>0.05) (*Figure 5A*). Furthermore, a remarkable positive correlation was found between FoxP3$^+$Tregs and AFP (r=0.927, 0.916, 0.818, 0.931, 0.944, and 0.910, respectively) in PB of groups A–F (P<0.05) (*Table 3*, *Figure 5C*).

VEGF concentration

There was significant increase of VEGF expression in group E compared with that in group F and drug therapy groups (P<0.01). The VEGF level in group A was reduced the most significantly (P<0.01) in comparison with the normal group and no SRL monotherapy groups, but no obvious difference was observed among no SRL monotherapy groups (P>0.05) (*Figure 5B*). Moreover, there was an obvious positive correlation between FoxP3$^+$Tregs and VEGF (r=0.850, 0.901, 0.944, 0.921, 0.932, and 0.842, respectively) in PB of groups A–F (P<0.05) (*Table 3*, *Figure 5C*).

VEGF IHC staining of liver nodes was significantly increased in group E, where it was mainly concentrated in tumor cells and the portal area. Furthermore, the positive staining rate was lower in group A, and that in the no SRL monotherapy groups was between that of groups A and E (*Figure 6*).

AKT-mTOR expression in cancer tissues

In comparison with the model rats (group E), SRL-based therapy did not reduce the expression of AKT but down regulated the level of p-AKT in cancer cells (*Figure 7*). Moreover, SRL-based therapy not only decreased the expression of mTOR, but also significantly reduced the level of p-mTOR (P<0.01). SRL-based therapy also down

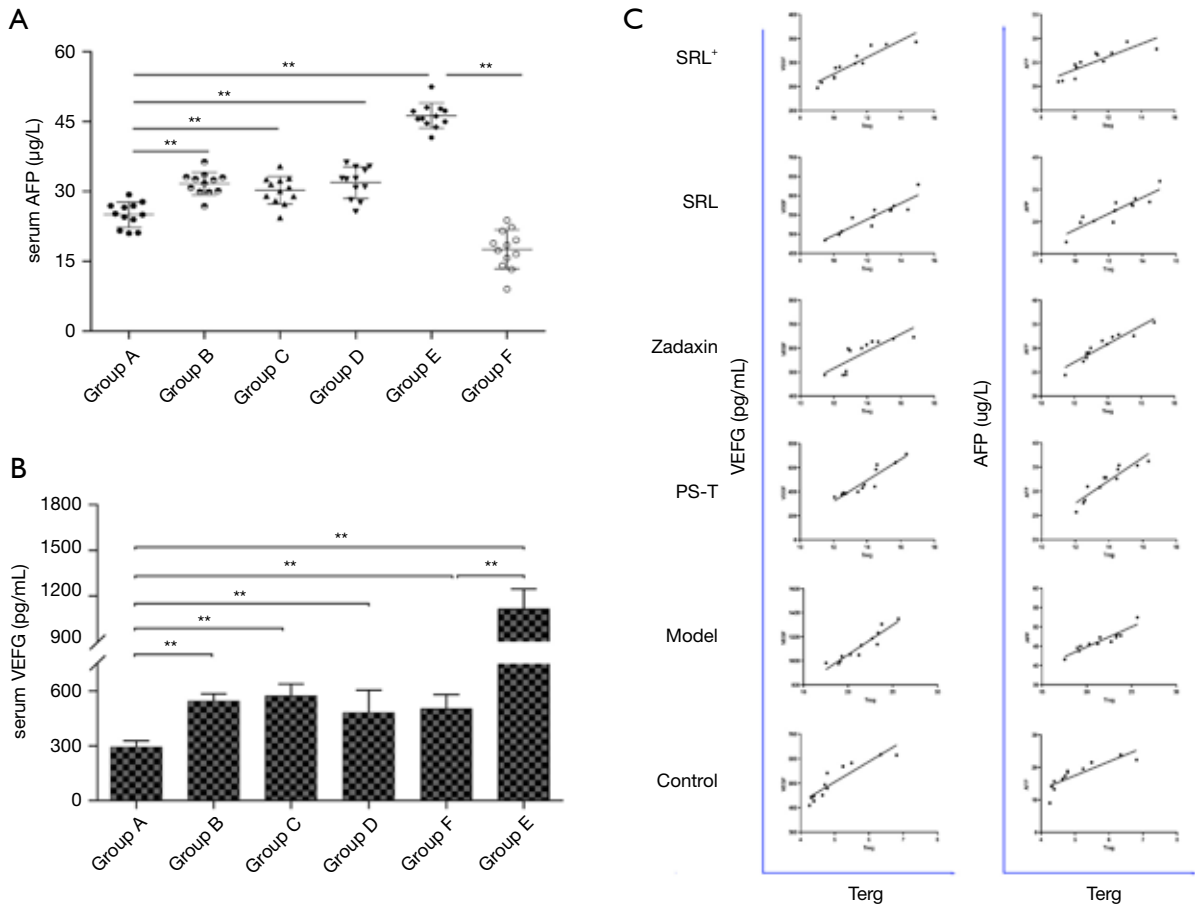

Figure 5 The serum level of AFP and VEGF in difference and the correlation analysis with FoxP3+Tregs. (A) Scatter diagram of AFP level analyzed with ANOVA (**P<0.01); (B) histogram of VEGF level analyzed with ANOVA (**P<0.01); (C) correlation analysis between FoxP3+Treg and AFP and VEGF in PB for each group (analyzed by Pearson, A–F respectively; P<0.05). group A, SRL-based therapy/SRL+; group B, SRL/RAPA; group C, Thymalfasin/Zadaxin; group D, Huaier extract/PS-T; group E, HCC model; group F, Blank/Control.

regulated p-AKT and p-mTOR compared with no SRL monotherapy (P<0.01) (*Figure 7A,B,C,D*).

IL-10 and TGF-β levels

Inhibitory cytokines IL-10 and TGF-β were significantly increased in group E (model rats) (P<0.01) compared with group F (Control group) (*Figure 7*). However, there were significant decreases after SRL-based therapy (P<0.01) in comparison with the model group (group E) and no obvious difference among no SRL monotherapy groups (P>0.05) (*Figure 7E,F*).

Survival analysis

The survival rate of rats in group A was significantly higher than that of rats in monotherapy groups and the model group. Mortality rates in group E were as high as 58.3% (7/12) with time of death ranging from 7 to 15 weeks after beginning treatments, and 33.3% of the rats displayed liver nodules that were demonstrated to be HCC except for one rat that died at 7 weeks and appeared to have cirrhosis based on HE staining results. Only one rat in group A died, which was delayed death at 15 weeks. Moreover, the mortality of rats in monotherapy groups was lower than that of group E and higher than that of group A, which was mainly at 12 weeks with slight pathological changes of liver lesions (*Figure 1B*). Survival benefit analysis suggested a significant difference between groups and demonstrated that SRL-based therapy significantly improved the survival of rats (P=0.02) (*Figure 8*).

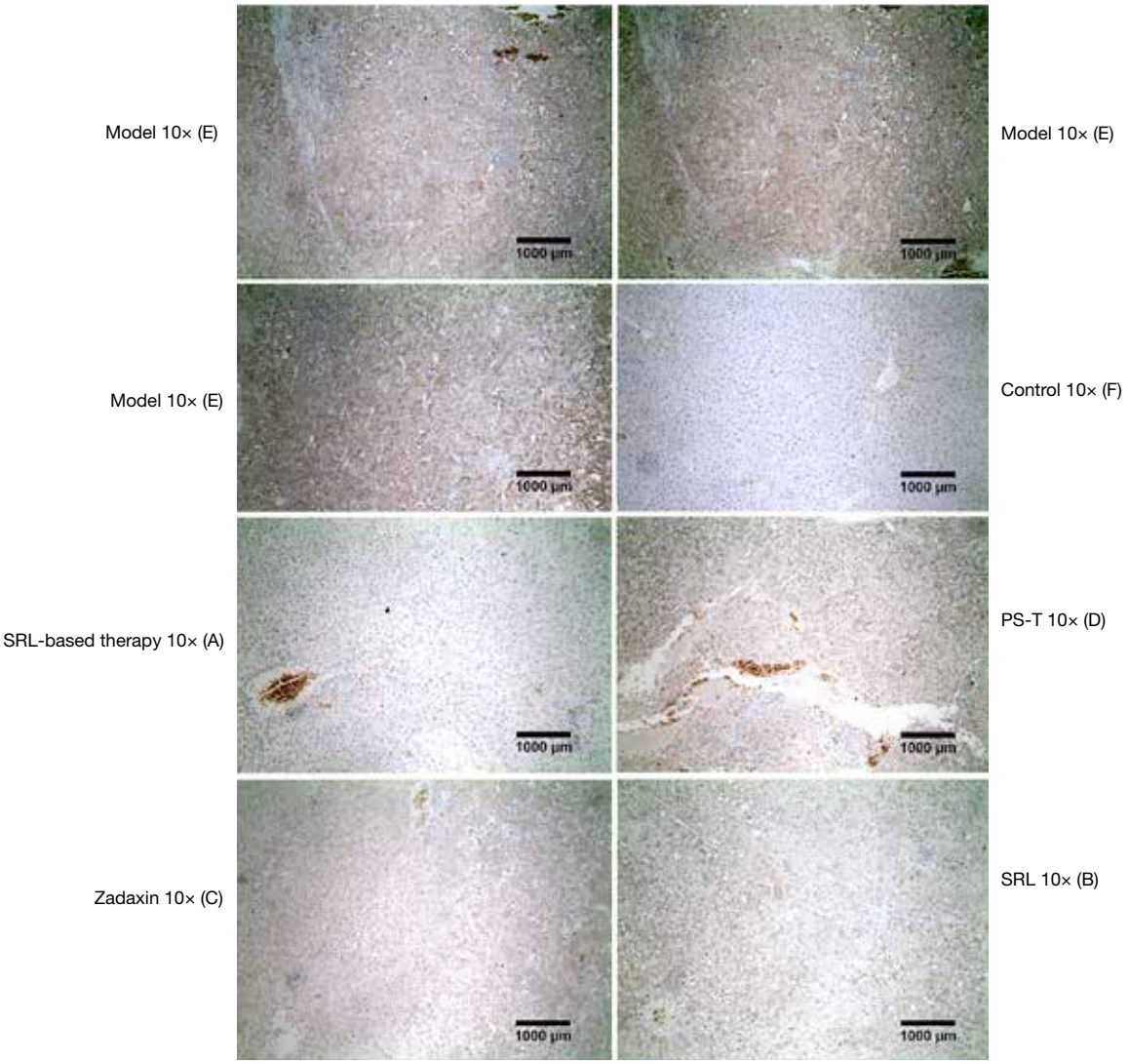

Figure 6 IHC stains results of VEGF expression. The results showed that VEGF expression was significantly increased in HCC model, mainly concentrated in the tumor cells and portal area. The positive staining rate was lower in other groups. Group A, SRL-based therapy; Group B, SRL/RAPR; Group C, Zadaxin; Group D, PS-T; Group E, Model; Group F, Control.

Discussion

Rat HCC model

The current rat model of LT cannot meet experimental needs well because of its low establishment rate, high mortality, instability, and long-term induction of tumor recurrence as well as the short survival time after LT. Through optimization and improvement of the modeling method reported previously (37-40) combined with verification through preliminary experiments, we developed an optimized chemical induction method with DEN and immunosuppression, which better simulates the characteristics of HCC recurrence after LT to provide an alternative rat model. At the experiment endpoint, most rats still displayed visible liver nodules. HE staining indicated that the normal liver lobule structure had disappeared with significant cell atypia, varied cell sizes and shapes, large and deeply stained nuclei, and a dense arrangement, which collectively demonstrated generation of HCC lesions and a successful tumor relapse model. Therefore, we believe that the rat model established by this method is completely feasible to fully meet research needs.

Table 3 the correlation ship of FoxP3$^+$Treg between VEGF and AFP of different groups

Groups	Treg and VEGF		Treg and AFP	
	r	P	r	P
Group A	0.927	0.000	0.850	0.000
Group B	0.916	0.000	0.901	0.001
Group C	0.818	0.001	0.944	0.000
Group D	0.931	0.000	0.921	0.000
Group E	0.944	0.000	0.932	0.000
Group F	0.910	0.000	0.842	0.001

Group A, SRL-based therapy group; Group B, Rapamycin/Sirolumus group; Group C, Thymalfasin group; Group D, Huaier extract group; Group E, HCC model group; Group F, Blank group.

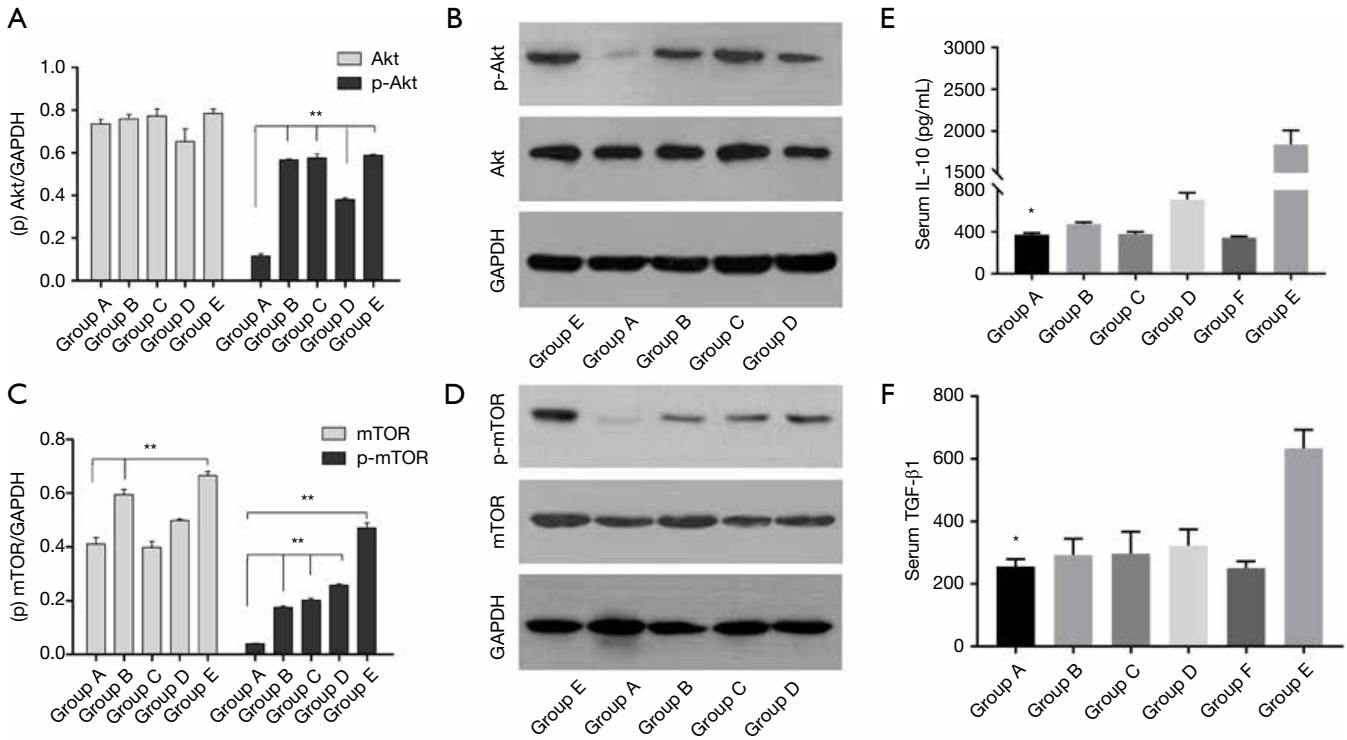

Figure 7 The expression of akt-mTOR protein (A,B,C,D) and inhibitory cytokines (E,F) in different groups. (A,B) The p-akt was decreased significantly in group A compared with other groups, **P<0.01; (C,D) the mTOR and p-mTOR all decreased significantly in group A compared with other groups, **P<0.01. (E) Histogram of IL-10 between different groups analyzed with ANOVA, obviously down-regulation in group A, *P<0.05; (F) histogram of TGF-β1 between different groups analyzed with ANOVA, remarkably down-regulation in group A, *P<0.05. group A, SRL-based therapy/SRL$^+$; group B, SRL/RAPA; group C, Thymalfasin/Zadaxin; group D, Huaier extract/PS-T; group E, HCC model; group F, Blank/Control.

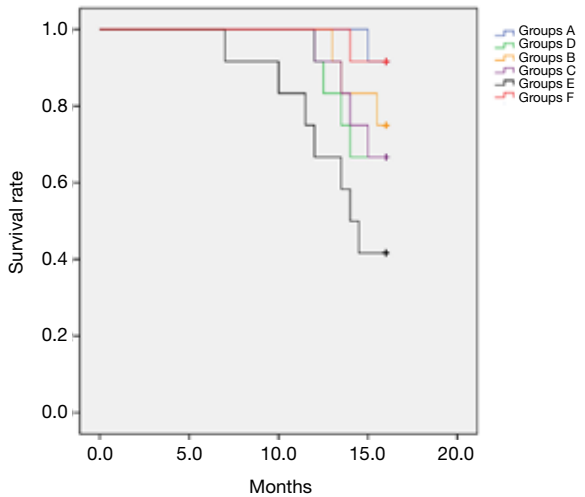

Figure 8 The survival rates and curve for different groups with Kaplan-Meier and log-rank analysis (P=0.02). group A, SRL-based therapy/SRL^{+}; group B, SRL/RAPA; group C, Thymalfasin/Zadaxin; group D, Huaier extract/PS-T; group E, HCC model; group F, Blank/Control.

Regulation of FoxP3^{+}Tregs and T cells

An increase of Foxp3^{+}Treg infiltration into hepatoma tissue, paracarcinoma tissue, and peripheral blood can inhibit the anti-tumor immune response and ability to recognize tumor antigens, which ultimately allows tumor cells to evade immune surveillance (13-15,41-43). Studies have reported an obvious negative correlation between high levels of FoxP3^{+}Tregs and a poor prognosis of HCC patients and a positive correlation between a high level of FoxP3^{+}Tregs and increased risk of tumor relapse (42,43). In this study, a higher FoxP3^{+}Treg level in PB and liver and spleen tissues resulted in a shorter survival time and poorer prognosis of rats.

Moreover, the level of FoxP3^{+}Tregs in PB was significantly higher in group E than in the SRL-based therapy group and no SRL monotherapy groups (P<0.05). The level of FoxP3^{+}Tregs was decreased significantly after SRL-based therapy (P<0.05) and no SRL monotherapy. This tendency was also observed in spleen and liver tissues. Therefore, a reduction of FoxP3^{+}Tregs maybe one of the underlying mechanisms that inhibits tumor growth and proliferation by SRL-based therapy.

FoxP3^{+}Tregs inhibit the activation and proliferation of effective T cells, especially CTLs, indirectly through inhibition of the secretion of cytokines IL-4, IL-10, or TGF-β (44-46) and directly through immediate contact with effective T cells, especially CTLs, upon release of cytotoxic cytokines (44-46). These indirect and direct immunosuppression effects contribute to induction of T cell immune suppression and immune incompetence that aid immune escape of cancer cells (34,35,47,48). In this study, expression of inhibitory cytokines IL-10 and TGF-β was promoted remarkably in the model rats, which declined significantly after SRL-based therapy. This change of IL-10 and TGF-β expression was in parallel with the change in FoxP3^{+}Tregs. These data indicated that down regulation of secreted cytokines IL-10 and TGF-β maybe a potential anti-tumor mechanism of FoxP3^{+}Tregs.

The correct balance of CD8^{+}T cells and other subgroups of T cells plays a crucial role in anti-tumor immunity (27,49). A balanced ratio between CD4^{+} and CD8^{+}T cells contributes to promotion of immunologic homeostasis, whereas its disruption accelerates the growth and proliferation of tumor cells (28-31,50-52). In this study, the levels of CD8^{+}T cells in PB of group E were significantly decreased compared with the normal group (P<0.05). However, the proportion of CD8^{+}T cells in PB of group A was obviously enhanced after SLR-based therapy. Expectedly, there was a negative correlation between FoxP3^{+}Tregs and CD8^{+}T cells or CD4^{+}/CD8^{+}T cells. CD8^{+}T cell levels in the liver and spleen were obviously higher after SRL-based therapy (P<0.05). Based on the changing trend of the T cell subgroup, the increased level of FoxP3^{+}Tregs might exert a suppressive effect on CD8^{+}T cells. This inhibitory action may be weakened by the treatment effect of SRL-based therapy.

Collectively, these data indicate that SRL-based therapy decreased FoxP3^{+}Tregs and weakened their inhibitory effect by reducing secreted inhibitory cytokines IL-10 and TGF-β, and ultimately enhanced the viability and number of CD8^{+}T cells to elicit an anti-tumor effect. However, the activation effect of the CD8^{+}T cells and the function of the effective T cells measured by granzyme B and others in this study not fully analysis which was the further study objective in the next experiments.

Regulatory mechanism of SRL-based therapy

Although positively of up to 81% AFP is extensively applied in diagnosis, treatment, prognosis, and tumor relapse (53), more attention should be focused on negativity of about 30% in HCC patients and false positive results due to its occurrence in hepatitis and other benign diseases. In this study, nearly all samples in group E were positive (98%) with levels obviously higher than the normal value (P<0.05).

The drug therapy downregulated AFP expression, which was most significant in the SRL-based therapy group (group A, P<0.05). Moreover, VEGF, which has a close relationship with HCC growth (54), is expressed at elevated levels in cancer tissue and PB of HCC patients (54,55). We have reported that a high level of FoxP3+Tregs is associated with a poor prognosis and high risk of tumor relapse during a 5-year follow-up (18). In the present study, we found a significant positive correlation between the expression levels of AFP and VEGF and an increase in FoxP3+Tregs. This suggests that FoxP3+Tregs can be used as a prognosis index for early HCC relapse when applied with AFP, because they can be easily detected in PB. Studies in China have also demonstrated that application of Huaier to HCC patients after LT reduces the expression of VEGF and prolongs survival time. VEGF monitoring may facilitate prognosis and detection of recurrence in HCC patients (24,56,57). A significant positive correlation of FoxP3+Tregs with AFP and VEGF were found in this study, and we believe that simultaneous assessment of AFP, FoxP3+Tregs, and VEGF should be considered useful in analysis the inhibitory effects of drugs on tumor cells and predict tumor recurrence.

Huaier (19) and SRL (58,59) both suppress the formation of new blood vessels in liver cancer tissue to inhibit tumor cell growth through downregulation of the VEGF level. Huaier also inhibits the tumorigenic capacity of cells through mTOR signaling and contributes to increased sensitivity of cells to rapamycin (22,24). Therefore, application of Huaier with RAPA might be a promising therapy for the treatment of HCC that is mainly caused by aberrant mTOR signaling. Furthermore, thymalfasin improves the cellular immunity of CTLs and affects FoxP3+Treg functions (60-62). Although there has been increasing research on its safety and efficacy in LT patients, whether thymalfasin functions by regulating the mTOR signaling pathway remains unknown. Our previous studies demonstrated an encouraging survival benefit of SRL-based therapy (18) by regulation of FoxP3+Tregs and CD8+T cells without rejection when applying Zadaxin (18,26). In this study, both SRL and Huaier reduced the expression of p-AKT and p-mTOR in the PI3K-AKT-mTOR signaling pathway of cancer cells. Thus, SRL-based therapy showed a prominent inhibitory effect. Moreover, the target molecule levels and pathological results (HE/IHC staining) showed the expected results with the VEGF level decreased significantly and cancer cell infiltration reduced remarkably. These results indicated that application PS-T and Zadaxin when accepting SRL therapy acts cooperativity to inhibit cancer growth and proliferation through the mTOR signaling path way which may be through increasing the activity of CD8+T cells for the anti-tumor response, and the SRL treatment effect of enhancement CD8+T cellular level with the PS-T and Zadaxin also needs to study in the further experiments.

Survival time of SRL-based therapy

Although Tacrolimus remains as a commonly used immunosuppressant, increasing studies and the International Multi-center Clinical Trial recommend rapamycin for liver transplantation of HCC patients because of its long-term survival benefits (17). Most experts agree with the first high-level evidence to select SRL-based immunosuppression for LT recipients with HCC.

SRL-based therapy in our center for terminal HCC patients after LT has shown long-term survival benefits and does not increase the rate of rejection or opportunistic infection when applied with Zadaxin (18,26). Application of Zadaxin is also safe and effective in LT patients with psoriasis (26). SRL-based therapy shows a survival benefit and disease control in comparison with Tacrolimus-based therapy.

The fewer rat liver lesions and most significant inhibitory effect on cancer cell growth in group A indicated that SRL-based therapy improves survival. The prognosis analysis suggested that the survival time of rats in group E was decreased obviously and mortality was increased significantly (P<0.05) compared with the other groups. When treated with SRL-based therapy, the survival time was obviously prolonged, death time remarkably delayed, and mortality was decreased significantly, but no SRL monotherapy was limited.

Conclusions

In this present study, by applying an optimized and improved chemical induction method, we successfully established a simulative rat model of HCC relapse after LT, which fully met the needs of this study. SRL-based therapy exerted an anti-tumor effect by reducing FoxP3+Tregs and their secreted inhibitory cytokines, which may ultimately enhance the viability and activities of CD8+T cells. SRL-based therapy inhibited cancer growth and proliferation through the AKT-mTOR signaling pathway, and the application PS-T and Zadaxin enhanced the synergistic effect of SRL. Furthermore, FoxP3+Tregs might be a useful

marker for early prognosis of HCC.

The effect of the combined therapy on FoxP3$^+$Tregs was mediated through the mTOR signaling pathway, and changes in the levels of other molecules are unclear, which need verification in a larger sample size and further *in vitro* experiments. Moreover, the effect of FoxP3$^+$Tregs depletion on CD8$^+$T cell in ret model was also needs further study.

Acknowledgments

We thank Gaitianli Medicine Co. Ltd., China for supplying the Huaier extract.

Funding: This study was supported by the Chao yang Scholar Program (1351 Talent Training Program, CYXZ-2017-10) and National Natural Science Foundation of China (81471590 and 81972568).

Footnote

Conflicts of Interest: All authors have completed the ICMJE uniform disclosure form (available at http://dx.doi.org/10.21037/atm.2020.03.129). The authors have no conflicts of interest to declare.

Ethical Statement: The authors are accountable for all aspects of the work in ensuring that questions related to the accuracy or integrity of any part of the work are appropriately investigated and resolved. All animal studies were conducted with the approval and guidance of the 8th Medical Center of the Chinese PLA General Hospital Medical Animal Ethics Committee. Animals were housed and treated in accordance with the Animal Welfare Act and Institutional Guidelines for the Care and Use of Laboratory Animals.

References

1. The Lancet. GLOBOCAN 2018: Counting the toll of cancer. Lancet 2018;392:985.
2. Feng RM, Zong YN, Cao SM, et al. Current cancer situation in China: Good or bad news from the 2018 Global Cancer Statistics? Cancer Commun (Lond) 2019;39:22.
3. Bray F, Ferlay J, Soerjomataram I, et al. Global cancer statistics 2018: GLOBOCAN estimates of incidence and mortality worldwide for 36 cancers in 185 countries. CA Cancer J Clin 2018;68:394-424.
4. Thomas MB, Jaffe D, Choti MM, et al. Hepatocellular carcinoma: Consensus recommendations of the National Cancer Institute Clinical Trials Planning Meeting. J Clin Oncol 2010;28:3994-4005.
5. Yao FY, Xiao L, Bass NM, et al. Liver transplantation for hepatocellular carcinoma: Validation of the UCSF-Expanded criteria based on preoperative imaging. Am J Transplant 2007;7:2587-96.
6. Piras-Straub K, Khairzada K, Gerken G, et al. Glutamate dehydrogenase and alkaline phosphatase as very early predictors of hepatocellular carcinoma recurrence after liver transplantation. Digestion 2015;91:117-27.
7. Dutkowski P, Linecker M, Deoliveira ML, et al. Challenges to liver transplantation and strategies to improve outcomes. Gastroenterology 2015;148:307-23.
8. Varona MA, Soriano A, Aguirre-Jaime A, et al. Risk factors of hepatocellular carcinoma recurrence after liver transplantation: Accuracy of the Alpha-Fetoprotein model in a Single-Center experience. Transplant Proc 2015;47:84-9.
9. Welker MW, Bechstein WO, Zeuzem S, et al. Recurrent hepatocellular carcinoma after liver transplantation - an emerging clinical challenge. Transpl Int 2013;26:109-18.
10. Pecchi A. Post-transplantation hepatocellular carcinoma recurrence: Patterns and relation between vascularity and differentiation degree. World J Hepatol 2015;7:276-84.
11. Tong Z, Liu L, Zheng Y, et al. Predictive value of preoperative peripheral blood neutrophil/lymphocyte ratio for lymph node metastasis in patients of resectable pancreatic neuroendocrine tumors: A nomogram-based study. World J Surg Oncol 2017;15:108.
12. Tang H, Li RP, Liang P, et al. MiR-125a inhibits the migration and invasion of liver cancer cells via suppression of the PI3K/AKT/mTOR signaling pathway. Oncol Lett 2015;10:681-6.
13. Mathai AM, Kapadia MJ, Alexander J, et al. Role of foxp3-positive tumor-infiltrating lymphocytes in the histologic features and clinical outcomes of hepatocellular carcinoma. Am J Surg Pathol 2012;36:980-6.

14. Du Y, Chen X, Huang ZM, et al. Increased frequency of Foxp3+regulatory T cells in mice with hepatocellular carcinoma. Asian Pac J Cancer Prev 2012;13:3815-9.
15. Lin SZ, Chen KJ, Xu ZY, et al. Prediction of recurrence and survival in hepatocellular carcinoma based on two cox models mainly determined by FoxP3+regulatory t cells. Cancer Prev Res (Phila) 2013;6:594-602.
16. Vivarelli M, Cucchetti A, Barba G L, et al. Liver transplantation for hepatocellular carcinoma under calcineurin inhibitors. Ann Surg 2008;248:857-62.
17. Geissler EK, Schnitzbauer AA, Zülke C, et al. Sirolimus use in liver transplant recipients with hepatocellular carcinoma. Transplantation 2016;100:116-25.
18. Zhou L, Pan LC, Zheng YG, et al. Novel strategy of sirolimus plus thymalfasin and huaier granule on tumor recurrence of hepatocellular carcinoma beyond the UCSF criteria following liver transplantation: A single center experience. Oncol Lett 2018;16:4407-17.
19. Chen L, Lu P, Lu Z, et al. Anticancer Effect of PS-T on the Experimental Hepatocellular Carcinoma. 2004;1:55-9.
20. Zhang N, Kong X, Yan S, et al. Huaier aqueous extract inhibits proliferation of breast cancer cells by inducing apoptosis. Cancer Sci 2010;101:2375-83.
21. Wang CY, Bai X, Wang C. Traditional chinese medicine: A treasured natural resource of anticancer drug research and development. Am J Chin Med 2014;42:543-59.
22. Hu Z, Yang A, Fan H, et al. Huaier aqueous extract sensitizes cells to rapamycin and cisplatin through activating mTOR signaling. J Ethnopharmacol 2016;186:143-50.
23. Yang AL, Hu ZD, Tu PF. Research progress on anti-tumor effect of Huaier. Zhongguo Zhong Yao Za Zhi 2015;40:4805-10.
24. Zhao J, Hu J, Cai J, et al. Vascular endothelial growth factor expression in serum of patients with hepatocellular carcinoma. Chin Med J (Engl) 2003;116:772-6.
25. Zimmerman MA, Trotter JF, Wachs M, et al. Sirolimus-based immunosuppression following liver transplantation for hepatocellular carcinoma. Liver Transpl 2008;14:633-8.
26. Zhou L, Du GS, Pan LC, et al. Sirolimus treatment for cirrhosis or hepatocellular carcinoma patients accompanied by psoriasis after liver transplantation: A single center experience. Oncol Lett 2017;14:7817-24.
27. Galon J. Type, density, and location of immune cells within human colorectal tumors predict clinical outcome. Science 2006;313:1960-4.
28. Ohwada S, Iino Y, Nakamura S, et al. Peripheral blood T cell subsets as a prognostic factor in gastric cancer. Jpn J Clin Oncol 1994;24:7-11.
29. Chen X, Du Y, Huang Z. CD4+CD25+Treg derived from hepatocellular carcinoma mice inhibits tumor immunity. Immunol Lett 2012;148:83-9.
30. Lee WC, Wu T, Chou H, et al. The impact of CD4+CD25+ T cells in the tumor microenvironment of hepatocellular carcinoma. Surgery 2012;151:213-22.
31. Huang Y, Liao H, Zhang Y, et al. Prognostic value of Tumor-Infiltrating FoxP3+ t cells in gastrointestinal cancers: A meta analysis. PLoS One 2014;9:e94376.
32. Thakur S, Singla A, Chawla Y, et al. Expansion of peripheral and intratumoral regulatory T-cells in hepatocellular carcinoma: A case-control study. Indian J Pathol Microbiol 2011;54:448.
33. Pons JA, Revillanuin B, Ramírez P, et al. Development of immune tolerance in liver transplantation. Gastroenterol Hepatol 2011;34:155-69.
34. Unitt E, Rushbrook SM, Marshall A, et al. Compromised lymphocytes infiltrate hepatocellular carcinoma: The role of T-regulatory cells. Hepatology 2005;41:722-30.
35. Yang XH, Yamagiwa S, Ichida T, et al. Increase of CD4+CD25+ regulatory T-cells in the liver of patients with hepatocellular carcinoma. J Hepatol 2006;45:254-62.
36. Karczewski M, Karczewski J, Kostrzewa A, et al. The role of foxp3+ regulatory t cells in kidney transplantation. Transplant Proc 2009;41:1527-9.
37. Rignall B, Braeuning A, Buchmann A, et al. Tumor formation in liver of conditional β-catenin-deficient mice exposed to a diethylnitrosamine/phenobarbital tumor promotion regimen. Carcinogenesis 2011;32:52-7.
38. Puatanachokchai R, Kakuni M, Wanibuchi H, et al. Lack of promoting effects of phenobarbital at low dose on diethylnitrosamine-induced hepatocarcinogenesis in TGF-alpha transgenic mice. Asian Pac J Cancer Prev 2006;7:274-8.
39. Newell P, Villanueva A, Friedman SL, et al. Experimental models of hepatocellular carcinoma. J Hepatol 2008;48:858-79.
40. Matsuzaki T, Murase N, Yagihashi A, et al. Liver transplantation for diethylnitrosamine-induced hepatocellular carcinoma in rats. Transplant Proc 1992;24:748-51.
41. Mougiakakos D, Choudhury A, Lladser A, et al. Regulatory T cells in cancer. Adv Cancer Res 2010;107:57-117.
42. Li F, Guo Z, Lizée G, et al. Clinical prognostic value of CD4+CD25+FOXP3+regulatory T cells in peripheral blood of Barcelona Clinic Liver Cancer (BCLC) stage B hepatocellular carcinoma patients. Clin Chem Lab Med

2014;52:1357-65.
43. Ozgur HH, Ercetin AP, Eliyatkin N, et al. Regulatory T cells and their prognostic value in hepatopancreatobiliary tumours. Hepatogastroenterology 2014;61:1847-51.
44. Câmara NOS, Sebille F, Lechler RI. Human $CD4^+CD25^+$ regulatory cells have marked and sustained effects on $CD8^+$ T cell activation. Eur J Immunol 2003;33:3473-83.
45. Casares N, Arribillaga L, Sarobe P, et al. $CD4^+/CD25^+$ regulatory cells inhibit activation of tumor-primed $CD4^+$T cells with IFN-gamma-dependent antiangiogenic activity, as well as long-lasting tumor immunity elicited by peptide vaccination. J Immunol 2003;171:5931-9.
46. Seo N, Yamashiro H, Tadaki T. Anti-infective and anti-tumor agents based on the depletion of immune suppressive effects. Curr Med Chem 2008;15:991-6.
47. Pedroza-Gonzalez A, Verhoef C, Ijzermans J N M, et al. Activated tumor-infiltrating $CD4^+$ regulatory T cells restrain antitumor immunity in patients with primary or metastatic liver cancer. Hepatology 2013;57:183-94.
48. Sharma S, Khosla R, David P, et al. $CD4^+CD25^+$CD127low regulatory t cells play predominant Anti-Tumor suppressive role in hepatitis b Virus-Associated hepatocellular carcinoma. Front Immunol 2015;6:49.
49. Pagès F, Galon J, Dieu-Nosjean M, et al. Immune infiltration in human tumors: A prognostic factor that should not be ignored. Oncogene 2010;29:1093-102.
50. Hiura T, Kagamu H, Miura S, et al. Both regulatory T cells and antitumor effector T cells are primed in the same draining lymph nodes during tumor progression. J Immunol 2005;175:5058-66.
51. Sasaki A, Tanaka F, Mimori K, et al. Prognostic value of tumor-infiltrating $FOXP3^+$ regulatory T cells in patients with hepatocellular carcinoma. Eur J Surg Oncol 2008;34:173-9.
52. Shang B, Liu Y, Jiang S, et al. Prognostic value of tumor-infiltrating $FoxP3^+$ regulatory T cells in cancers: A systematic review and meta-analysis. Sci Rep 2015;5:15179.
53. Marrero JA, Feng Z, Wang Y, et al. A-Fetoprotein, des-γ carboxyprothrombin, and Lectin-Bound α-Fetoprotein in early hepatocellular carcinoma. Gastroenterology. 2009;137:110-8.
54. Torimura T, Sata M, Ueno T, et al. Increased expression of vascular endothelial growth factor is associated with tumor progression in hepatocellular carcinoma. Hum Pathol 1998;29:986-91.
55. Salven P, Orpana A, Joensuu H. Leukocytes and platelets of patients with cancer contain high levels of vascular endothelial growth factor. Clin Cancer Res 1999;5:487-91.
56. Lee JK, Hong YJ, Han CJ, et al. Clinical usefulness of serum and plasma vascular endothelial growth factor in cancer patients: Which is the optimal specimen? Int J Oncol 2000;17:149-52.
57. Jinno K, Tanimizu M, Hyodo I, et al. Circulating vascular endothelial growth factor (VEGF) is a possible tumor marker for metastasis in human hepatocellular carcinoma. J Gastroenterol 1998;33:376-82.
58. Toso C, Merani S, Bigam D L, et al. Sirolimus-based immunosuppression is associated with increased survival after liver transplantation for hepatocellular carcinoma. Hepatology 2010;51:1237-43.
59. Panwalkar A, Verstovsek S, Giles FJ. Mammalian target of rapamycin inhibition as therapy for hematologic malignancies. Cancer 2004;100:657-66.
60. Garaci E, Pica F, Matteucci C, et al. Historical review on thymosin α1 in oncology: Preclinical and clinical experiences. Expert Opin Biol Ther 2015;15:S31-9.
61. Garaci E, Pica F, Serafino A, et al. Thymosin α1 and cancer: Action on immune effector and tumor target cells. Ann Ny Acad Sci 2012;1269:26-33.
62. Serafino A, Pierimarchi P, Pica F, et al. Thymosin α1 as a stimulatory agent of innate cell-mediated immune response. Ann Ny Acad Sci 2012;1270:13-20.

Cite this article as: Zhou L, Pan LC, Zheng YG, Zhang XX, Liu ZJ, Meng X, Shi HD, Du GS, He Q. Reduction of $FoxP3^+$ Tregs by an immunosuppressive protocol of rapamycin plus Thymalfasin and Huaier extract predicts positive survival benefits in a rat model of hepatocellular carcinoma. Ann Transl Med 2020;8(7):472. doi: 10.21037/atm.2020.03.129

